

Twirling Sculptures

ERGUN AKLEMAN*

Texas A&M University, College Station, TX 77843

(Received 00 Month 200x; revised 00 Month 200x; in final form 00 Month 200x)

In this paper, I outline a method for constructing aesthetically pleasing sculptures containing spiral shapes. Since every face of an orientable manifold mesh can be given a consistent edge rotation ordering, if one applies an extrusion operator to each face of an orientable manifold mesh using the same rotation and scaling factors, each edge in the original mesh will be converted to an S-shaped region that consists of two spiral arms. The twirling nature of my sculptures results from these S-shaped regions. The final sculptures are obtained by smoothing the resulting shapes with a subdivision scheme. I discuss several methods for visually emphasizing the twirling nature of S-shaped regions. All the models and virtual sculptures in this paper are created using the Topological Mesh Modeling system TopMod .

Keywords: Topology, Manifold, Sculpture, Rind Modeling, Subdivision.

AMS Subject Classification: 57M99, 00A08

1. Introduction and Motivation

I believe the development of new methods to create new aesthetic forms is essential in any artistic application. With the help of computer graphics, many artists and scientists are now able to develop computational methods that use mathematics as a tool to create new aesthetic forms. And nowadays scientists/artists not only discover new methods, they also disseminate their findings.

Sculpting is one of the art forms that has been greatly influenced by these developments. One of the most exciting aspects of sculpting is the development of new methods to design and construct unusual, interesting, and aesthetically pleasing shapes. Contemporary sculptors such as Charles Perry [25], George Hart [20], Helaman Ferguson [14, 15], Bathsheba Grossman [17], Rinus Roelofs [27] and Carlo Séquin [29] have all contributed to this endeavor by combining art and mathematics to create unusual sculptures.

In this paper, I present a new approach to creating aesthetically pleasing sculptural forms. Using my approach it is possible to create a wide variety of virtual shapes. Some of these shapes do not resemble any existing sculptural or architectural forms. The resulting shapes can be physically realized with layered manufacturing techniques as shown in Figure 1. Some of the intermediate forms used to create twirling sculptures resemble Charles Perry's sculptures [25]. I also feel that many of my final twirling sculptures are conceptually related to the sculptures of Bathsheba Grossman [17] due to their high genus.

All the schematic diagrams, models and virtual sculptures shown in this paper were made using the Topological Mesh Modeling system TopMod [34]. Two versions of the system are freely available at <http://www-viz.tamu.edu/faculty/ergun/research/topology/download.html> and <http://www.topmod3d.org>. The publications related to TopMod are all freely available from my website at <http://www-viz.tamu.edu/faculty/ergun/research/topology/>.

*Corresponding author. Email: ergun@viz.tamu.edu, phone: (979) 845 6599, fax: (979) 845 4491



Figure 1. Two photographs of the first twirling sculpture I designed. This physical realization of the virtual twirling sculpture was made from ABS plastic and printed using a Fused Deposition Modeling (FDM) Machine. It was subsequently painted using acrylic paint. The circumradius of this sculpture is 5.5cm.

2. Spirals and S-shaped Double Spirals

Twirling sculptures are the result of applying an operation that transforms an existing shape into a new shape consisting of 3D spiral forms. I feel that the aesthetic beauty of twirling sculptures comes from these 3D spiral forms.

Spirals are one of the most common shapes found in nature, mathematics, and art [8, 11, 21, 37]. Spiral shapes lie behind the beauty of many natural objects including snails shells, seashells and rams' horns [32]. We even have a spiral in our body; the cochlea in our inner ear is spiral shaped. Many galaxies (including our own Milky Way) are spiral shaped. Some people say that the galaxies are beautiful because of their spiral shapes [16]. Some galaxies consist of two spirals arranged in an S-shape [35]. S-shaped spirals can also be observed when mixing two fluids.

Spiral forms exist in almost all cultures as artistic and mystical symbols. We see S-shaped double spirals in Stone Age art. Celtic crosses have whorls. Spirals can be found in Greek votive art and Tribal tattoos [21]. This widespread usage of the spiral form may imply that humans innately find them aesthetically pleasing and interesting.

Spirals are popular in mathematics. They are among the most studied curves since ancient Greek times. Although spirals are usually represented by parametric equations, there are a wide variety of methods that can be used to construct and represent spirals. There are also many named spirals such as the Archimedean spiral, the Fermat spiral, the Logarithmic spiral, Fibonacci spiral, Euler and Cornu spirals [11, 21, 37]. Spirals even appear when we zoom in on the Mandelbrot and Julia sets [23]. Spiral forms are used by Charles Perry [25] in his mathematically inspired sculptures. Daniel Erdely's Spidrons also exhibit spiral structures in 3D [12, 13].

My spiral construction arises from successive rotation and scaling of regular polygons in such a way that it resembles the construction of pursuit curves [26, 30]. For pursuit curves, consider the operation of scaling and rotating a square by a fixed angle around its center such that its corners touch the sides of the original square. Successive application of this operation creates a set of nested squares. The corners of successively created nested squares form four spiral arms. As the rotation angle gets smaller and smaller, the spiral arms converge to a logarithmic spiral. The procedure scaling and rotating can be applied to any polygon. Even though for most non-regular polygons the resulting shapes may not be perfect spirals, we can still visually obtain a spiral look. Therefore, by rotating and scaling the faces of a polyhedron, it is straightforward to create spirals in 3D. The next section shows that it is easy to make these spirals S-shaped using the manifold property of polyhedral meshes.

3. Manifold Meshes and S-shaped Double Spirals on Manifold Meshes

A 2-dimensional manifold, or simply 2-manifold, is a topological space that is locally Euclidean (i.e., around every point, there is a neighborhood that is topologically the same as the open unit ball in \mathbb{R}^2) [33]. A 2-manifold mesh can be non-orientable and orientable 2-manifold meshes can have self-intersections. Therefore, 2-manifolds may not always be physically realizable. Since, my goal is to create S-shaped double spirals as physically realizable shapes, I consider only orientable 2-manifolds in \mathbb{R}^3 without self-intersection, which are usually called surfaces [38] that can represent a physical body of arbitrary genus.

In our software, 2-manifold surfaces can be represented with the combinatorial structure of a graph and an associated "rotation system" [2, 4, 10, 24]. However, that is not necessary to understand the following, because the geometry of our starting polyhedra can be represented with a standard "half-edge" data structure [24]. In half-edge data structure, every edge will be represented by two half-edges pointing in opposite directions (See Figure 2). More importantly for this paper, the boundary of every face is described with a cyclically ordered sequence of half-edges, which can be considered as n vectors going around the face in consistent order (all clockwise or all counter-clockwise) as seen from the outside of the solid. This consistent order is the key to creating S-shaped spirals.

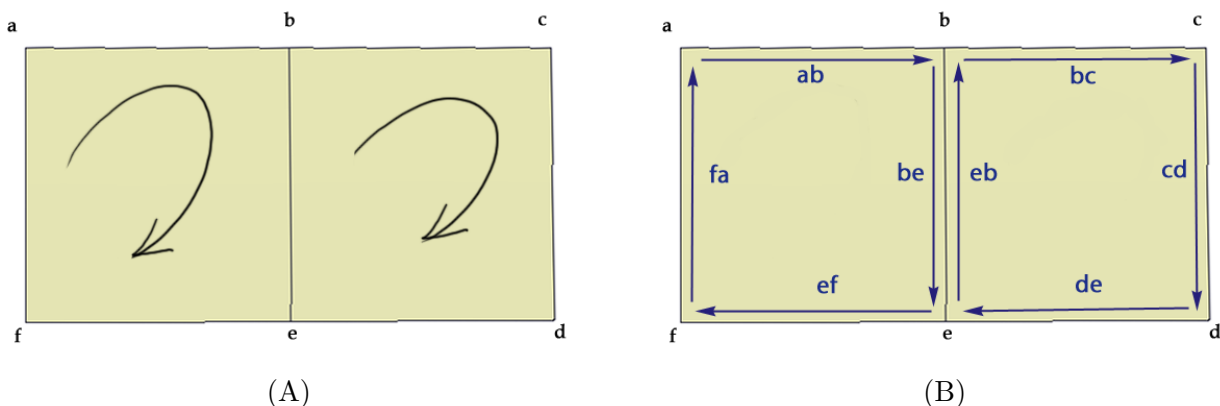


Figure 2. (A) shows two faces of a manifold mesh that share an edge. In the 2-manifold mesh, these faces are represented as two cyclically ordered sets $f_1 = \{a, b, e, f\}$ and $f_2 = \{b, c, d, e\}$. Here, the cyclic ordering corresponds to clockwise rotation. Note how the cyclic orders are consistent. The same shared edge appears as $\{b, e\}$ in f_1 and $\{e, b\}$ in f_2 . This is to be expected if one is to have a consistent rotation order in each face [2]. The two instances of the same edge are called half-edges. (B) shows the half-edges of these two faces.

As we noted in previous section, if we rotate and scale faces that are formed by straight line segments in 3D space around the center of each polygonal face of a 2-manifold mesh, we obtain k spiral arms for each k -sided face. If this operation is applied to every face of a 2-manifold mesh consistent with its rotation system, these spiral arms form S-shaped double spirals. Figure 3 shows that if we rotate and scale two faces that share an edge in a 2-manifold mesh, the rotated and scaled version of the shared edge creates S-shaped regions that consist of two spiral arms. Figure 5 shows S-shaped spiral regions on regular polyhedra.

Our problem is that we cannot simply rotate and scale the faces of an orientable 2-manifold mesh as this will create a large number of disconnected faces that will not represent any physically realizable shape. The simple solution is to use extrusion while performing successive rotations and scalings of the faces.

4. Extrusion Operations

An extrusion is a local operation that can be applied to one face of a mesh without affecting the others. Classical extrusion, which pastes a prism to a face, is an under-rated yet commonly-used operator in 3D modeling. This operation is called 'cubical extrusion' in TopMod [22, 34], since it can create a cube-shaped extrusion when applied to a square face. Assume that a polygon lies in the xy -plane. With cubical extrusion, a positive z -component is added to all vertices, so that the original polygon gets lifted up to the corresponding z -height. For each of the edges of the polygon a rectangle is added which connects the

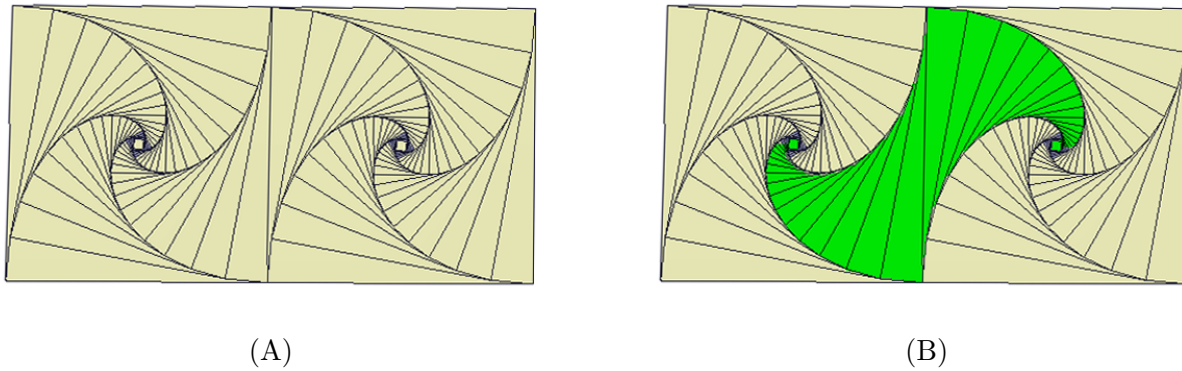


Figure 3. In a 2-manifold mesh, if we rotate and scale two faces that share an edge, the rotated and scaled version of the shared edge creates S-shaped regions that consist of two spiral arms. (A) shows the spirals that are created by rotating and scaling f_1 and f_2 shown in Figure 2 according to the rotation direction of each face. (C) shows that rotation and scaling of half edges $\{b, e\}$ and $\{e, b\}$ create two spirals that form an S-shape.

old and the new positions of these polygon edges. To generalize this operation we may uniformly scale the lifted polygon and possibly even rotate it around a vertical axis through its centroid. With the advent of the Catmull-Clark [7] and Doo-Sabin [9, 28] subdivision schemes, which work best with quadrilateral control meshes, cubical extrusion became more important, since it produces quadrilaterals when applied to quadrilateral meshes. I now formally introduce cubical extrusion.

Let f be an N -sided face given as an ordered set of vertex positions in 3D, $f = \{\mathbf{v}_0, \dots, \mathbf{v}_i, \dots, \mathbf{v}_{N-1}\}$ where $\mathbf{v}_i = (x_i, y_i, z_i)$. An extrusion operation applied to f creates a new n -sided face f' with vertex positions, $f' = \{\mathbf{v}'_0, \dots, \mathbf{v}'_i, \dots, \mathbf{v}'_{N-1}\}$. The difference between extrusion operations is in how the faces f and f' are connected. For cubical extrusion, we insert edges between pairs of vertices $\{\mathbf{v}_i, \mathbf{v}'_i\}$ by creating N quadrilateral faces $q_i = \{\mathbf{v}_i, \mathbf{v}_{i+1}, \mathbf{v}'_{i+1}, \mathbf{v}'_i\}$ where $+$ is the modulo N addition operator. Note that the faces f and f' and the q_i 's are not required to be planar or convex. Our equations used to compute $\{\mathbf{v}'_0, \dots, \mathbf{v}'_i, \dots, \mathbf{v}'_{N-1}\}$ must be general enough to provide an acceptable result for all possible cases. To derive such equations, we assume that for each $f = \{\mathbf{v}_0, \dots, \mathbf{v}_i, \dots, \mathbf{v}_{N-1}\}$ there is an approximating plane with normal vector \mathbf{n} originating from a center position \mathbf{v}_c . The normal vector \mathbf{n} is used as the direction of extrusion. If a face is planar, the estimation of \mathbf{n} must coincide with the normal to the plane of the face. Similarly, for rotation and scaling we have to estimate a center/pivot point \mathbf{v}_c . For a regular polygon, our computation must guarantee that \mathbf{v}_c is the center of the face. For a general face, \mathbf{v}_c must lie inside the convex hull defined $\{\mathbf{v}_0, \dots, \mathbf{v}_i, \dots, \mathbf{v}_{N-1}\}$. We use the following equations to estimate the vectors \mathbf{n} and \mathbf{v}_c . Let

$$\mathbf{v}_c = \sum_{i=0}^{N-1} \frac{\mathbf{v}_i}{N},$$

$$\mathbf{n} = \sum_{i=0}^{N-1} \frac{(\mathbf{v}_i - \mathbf{v}_c) \times (\mathbf{v}_{i+1} - \mathbf{v}_c)}{|(\mathbf{v}_i - \mathbf{v}_c) \times (\mathbf{v}_{i+1} - \mathbf{v}_c)|},$$

where \times is vector cross product. Vectors \mathbf{n} and \mathbf{v}_c will be used to compute the \mathbf{v}'_i positions. In practice, our \mathbf{v}'_i positions are controlled with a set of real-valued control parameters. In this paper, we focus on only three of these control parameters: the scaling factor s , the rotation angel θ and the displacement distance h . Using these three control parameters the \mathbf{v}'_i positions are computed by first scaling and rotating the face f around the vector \mathbf{n} and center point \mathbf{v}_c using s and θ and then translating the rotated and scaled face in the direction of the vector \mathbf{n} by a distance of h .

We now can analyze the situation where we apply a sequence of elementary cubical extrusions as de-

scribed above to each face. Let h_n , s_n , θ_n be the values of h , s and θ applied to each face during the n^{th} step of the sequence.

4.1. Non-Planar Extruded Spirals

Here, I analyze two cases that create non-planar extruded spirals for meshes with planar faces. For the sake of simplicity, assume $0 \leq s_n \leq 1$, all the s_n are equal, and all the θ_n are equal.

- All the h_n 's are positive and equal:

If the polygonal mesh is a convex shape and all faces are planar, regardless of the values of h_n , there will be no self-intersection of faces. As shown in Figure 4, the successive application of extrusions with h_n , θ and s_n constant will create structures that have an exponentially decreasing profile reminiscent of the Eiffel tower.

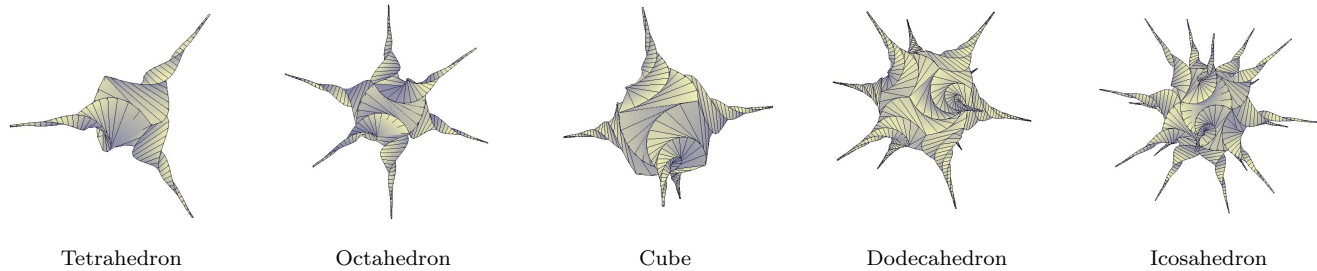


Figure 4. Platonic solids with 20 cubical extrusions. Here h and θ are small.

- The h_n 's are positive, but are not equal:

If we want to have finer control of the resulting shape of successive extrusions, one possible option is to change the value of h in each successive application of extrusion. For example, if $h_n = s_n^a h_{n-1}$, then the value of a becomes a parameter that allows users to control the shape of an idealized silhouette. For $a = 1$ the silhouette of the extrusion becomes a triangle and other values give a concave or convex silhouette.

4.2. Cubical Extrusions without Displacement

If we choose all $h_n = 0$, rotation and scaling alone creates un-extruded (i.e. flat) spiral regions. The characteristics of those spiral regions depend on the planarity and regularity of the face.

If all the faces are planar and regular, setting all $h_n = 0$ corresponds to pursuit curves [26, 30]. Pursuit curves require that the vertices of the rotated polygon touch the edges of the original polygon. Although we do not need such a strong requirement for our applications, it is possible to compute the relationship between s and θ needed to satisfy this condition for regular planar polygons. Using trigonometry it can be shown that the relationship between s and θ that meets this criterion for regular n -sided polygons is

$$s = \frac{1}{\cos \theta + \tan \frac{\pi}{n} \sin \theta} \quad (1)$$

where θ must be smaller than π/n . If we use values of s larger than the one given by equation 1, the polygons will intersect. Therefore, in practice it is better to use a value slightly smaller than the one in equation 1 (see Figure 5 for examples).

For non-regular and/or non-planar faces, it is not straightforward to obtain a simple equation similar to equation 1. For such cases, I find suitable values for s by trial and error. This can be done very quickly. Some examples for non-regular and non-planar cases are shown in Figure 6.

If all faces are planar and the value of h used for each face is zero, then all the spirals will be drawn in the same plane as the faces. If the faces are not all planar, or $h \neq 0$, the spirals will not be planar.

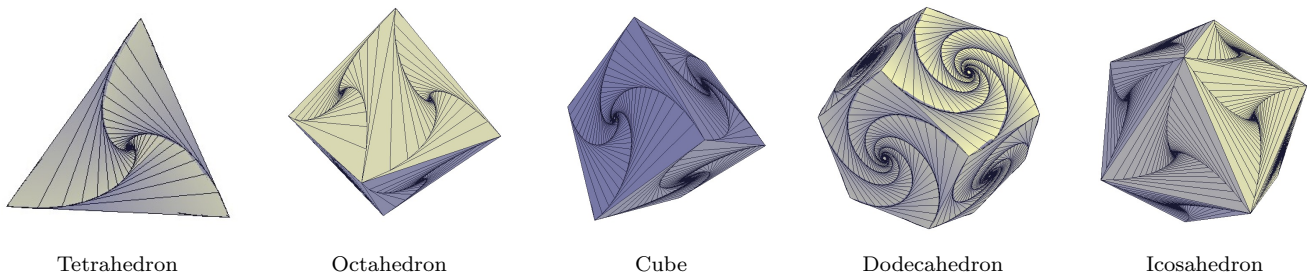


Figure 5. If we rotate and scale every regular polygonal face of a platonic solid, we can create S-shaped regions that consists of two spiral arms. It is interesting to note that the icosahedral shape resembles Icosaspirale, a 7 foot Bronze sculpture completed in 1966 by Charles Perry [25] that is located in front of the Alcoa Building in San Francisco.

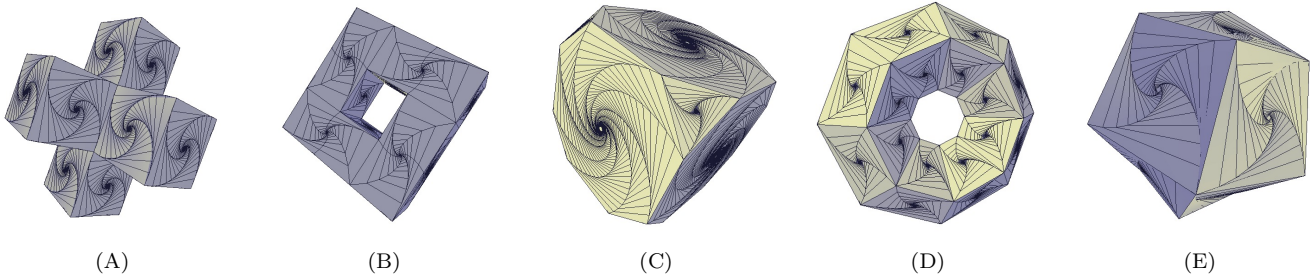


Figure 6. (A): Spirals on non-regular meshes with regular planar faces. (B), (C) and (D): Spirals on a mesh with non-regular planar faces. (E): Spirals on meshes with non-regular and non-planar faces.

4.3. Other Cases

I will not consider the cases where h_n is negative or $s_n > 1$ since it is possible to create self intersections with successive extrusions in these cases even when applied to convex planar meshes.

I have discovered a particularly interesting case (see Figure 7) in which the shapes are obtained by moving the vertices of extruded spiral shapes to a unit sphere. Note that this operation can only be applied to convex shapes. In this case, although all the vertices are on the unit sphere, the surfaces themselves are not on the sphere. Also note that even though the edges are straight, the final shape is twisty and non-convex like a hyperboloid. However, the resulting shapes are not guaranteed to be ruled surfaces. These particular structures visually remind me of Charles Perry’s Eclipse [25], a 35 foot aluminum sculpture inside the atrium of the Hyatt Regency Hotel, Embarcadero Center, San Francisco.

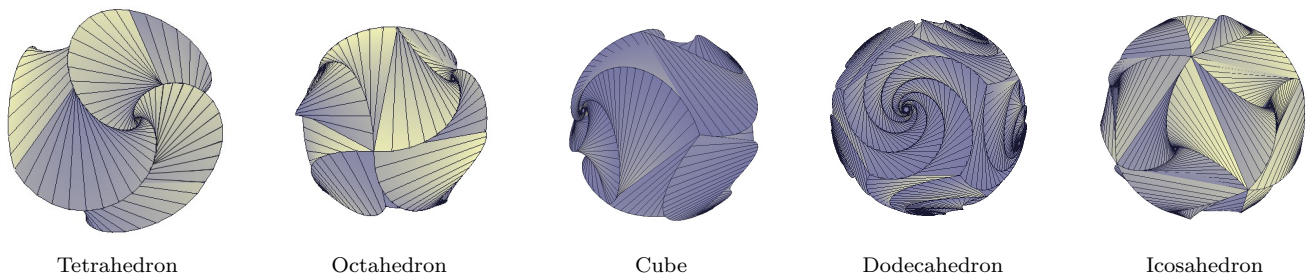


Figure 7. Interesting spirals obtained by moving vertices to a sphere.

5. Making S-shaped Regions More Visible

When we are dealing with the special case where all $h_n = 0$ yielding examples such as the ones in the Figures 5 and 6, S-shaped regions are visible only because we see the underlying mesh structure. If we

print these shapes using a 3D printer, nothing will be visible. This is not limited to the $h_n = 0$ case. For many cases S-shaped regions will be invisible without showing underlying mesh structure. I have identified one direct and two indirect approaches for making S-shaped regions visible in physical sculptures.

5.1. The Direct Approach

In the direct approach, S-shaped regions can be made visible in three different ways.

- (i) One can color S-shaped regions as shown in Figure 8(A).
- (ii) One can extrude groups of S-shaped regions as shown in Figure 8(B).
- (iii) One can open S-shaped holes as shown in Figure 8(C).

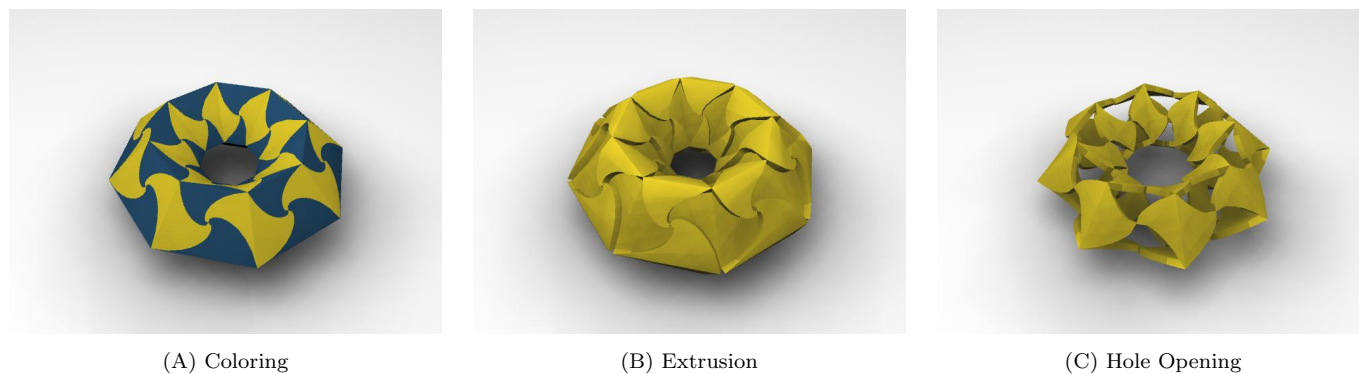


Figure 8. To make S-shaped regions visible we can either (A) color S-shaped regions, or (B) extrude S shaped regions as a group, or (C) open S-shaped holes. These are virtual sculptures that are rendered using commercial 3D modeling and animation software.

Coloring is very useful and can provide good results. However, coloring can be considered a painting solution not a modeling solution. For that, we need a shape based approach.

Both extrusion and hole opening are sculptural solutions for making S-shaped regions visible. Unfortunately, we cannot always make S-shaped regions visible using extrusion or hole opening. The problem is that both approaches are mathematically equivalent to the coloring of S-shaped regions using only two colors, and not all meshes can be colored with two colors. Moreover, no genus-zero mesh with S-shaped regions can be colored with two colors. Since S-shaped regions are derived from the edges of the initial mesh, this problem is related to an edge coloring problem [36]. Coloring S-shaped regions with only two colors requires that all valences and face orders of the initial mesh be divisible by 2. It is well known consequence of Euler's formula that for any genus-0 manifold mesh the number of 3-sided faces plus the number of 3-valence vertices is at least eight [18], so the valences and face orders can not all be even. In other words, we cannot two-color S-shaped regions on genus-0 surfaces. Therefore, we cannot open S-shaped holes on genus-0 surfaces.

Fortunately, for genera larger than zero, there exist manifold meshes in which all valences and face orders are even numbers that are greater than or equal to 4. A simple example is the toroidal shape that is shown in Figure 8. However, in general it is hard to find interesting meshes for which all valences and face orders are even numbers. I also feel that even for the ones in which all these are even numbers, the resulting sculptures may not look interesting. To understand where this feeling comes from, compare the images in Figure 8. In my opinion, the simple coloring in (A) is more interesting than the sculpture in (C). Fortunately, there are two "indirect" approaches for making spirals visible that do meet my criteria for aesthetically pleasing sculptures.

5.2. The Indirect Approach using Remeshing

One indirect approach is to isolate S-shaped regions by separating them with buffer zones. In this way, all S-shaped regions can have one color and all buffer zones can have another color. As a result, we can color

the resulting mesh with two colors.

To implement this idea, we need an operation that can automatically create buffer zones and isolate S-shaped regions. Fortunately, there exists a remeshing operation, called “Corner Cutting”, that automatically creates buffer zones [5]. “Corner Cutting” is a generalization of the polyhedral operation called “Mrs. Stott’s Expansion” (also called *expanding* in Conway notation) applied to manifold meshes [19]. A corner cutting remeshing operation converts any existing edge to a quadrilateral, any valence m vertex to an m -sided face, while original n -sided faces remain n -sided faces that are reduced to smaller versions of themselves. In other words, if there exists a region that consists of a set of faces, the edges and vertices at the boundary of that region are converted to a buffer zone.

There exists a variety of corner cutting schemes. Among them the Doo-Sabin subdivision is particularly useful [9]. The Doo-Sabin subdivision scheme is a special type of corner cutting scheme that creates a nice mesh structure after only a few applications [5]. Moreover, with successive applications of the Doo-Sabin scheme, the surface approaches a piecewise quadratic B-spline surface [9]. In this paper, I am not interested in the limit behavior of the Doo-Sabin scheme, but it is important to point out that just a few applications of the Doo-Sabin subdivision scheme can transform even extremely non-planar and non-convex faces to convex, almost planar faces [5]. In addition, only a few applications of the scheme are sufficient to achieve a visually smooth looking surface [5]. As a result, Doo-Sabin subdivision can be used to smooth the mesh while simultaneously isolating S-shaped regions and creating buffer zones (See Figures 9 and 10).

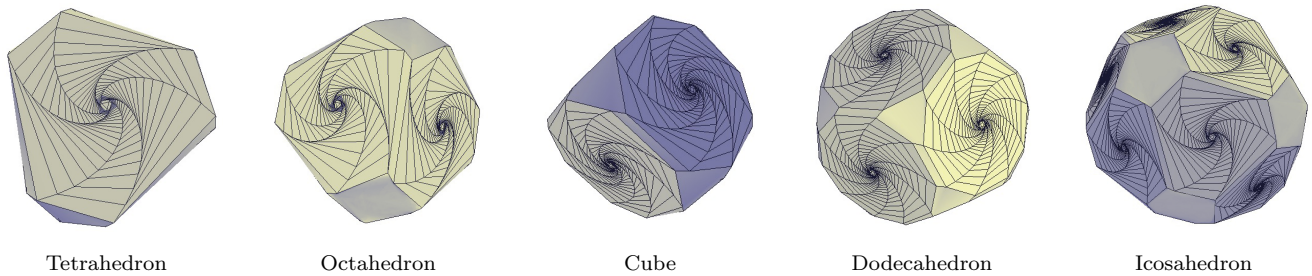


Figure 9. the Platonic solids from Figure 5 after one iteration of Doo-Sabin subdivision. S-shaped spiral regions become much more visible and buffer zones that consist of m spiral shaped arms appear, where m is the valence of the vertices of the initial mesh.

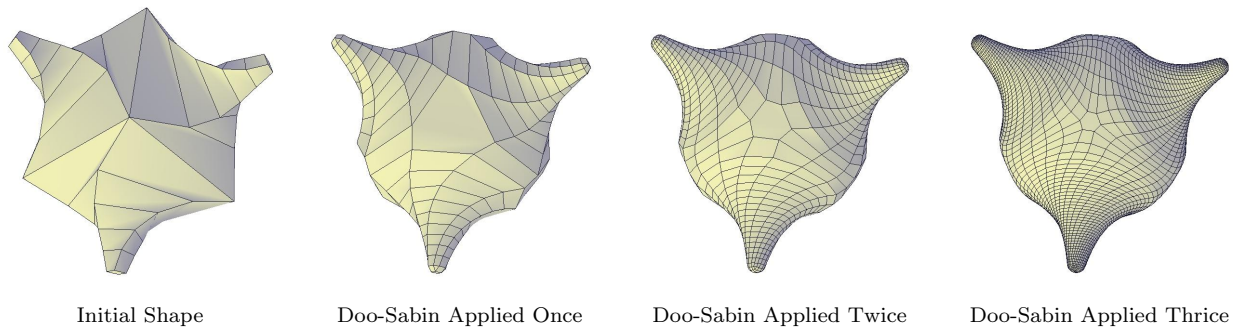


Figure 10. An extruded platonic solid after several applications of Doo-Sabin subdivision. Note that more S-shaped spiral regions appear after each application of Doo-Sabin subdivision.

6. Rind Modeling: the Indirect Approach of Opening Holes to Make S-shaped Regions Visible

When creating physical sculptures, I prefer to use Doo-Sabin subdivision followed by “hole opening” using Rind modeling [6]. I have already shown that one can always create S-shaped regions that can be colored by two colors using Doo-Sabin subdivision. Therefore, it is always possible to create isolated S-shaped regions. Once these regions are created, it is then easy to open holes using Rind modeling [6].

Rind modeling consists of two steps: in the first (automated) step, for any given 2-manifold mesh surface an offset surface is created based on a user defined thickness parameter. The second interactive step is hole punching or hole opening. Holes are punched by single mouse clicks on faces. By punching holes in each face of an S-shaped region, we can completely peel that region. I apply either the Doo-Sabin or the Catmull-Clark subdivision to the final manifold mesh to obtain a smoother surface.

Figure 11 shows a set of twirling sculptures in which S-shaped regions are made visible by opening holes. I have designed the initial 2-manifold meshes using a variety of mesh operations that are provided by TopMod [34]. To create final twirling sculptures I followed the procedure outlined in this paper. I have also tested this procedure in my computer aided sculpting course [1] and observed that, using extrusions, students can create a wide variety of interesting shapes. Despite their differences these sculptures have similar conceptual forms that resemble the virtual sculptures shown in this paper.

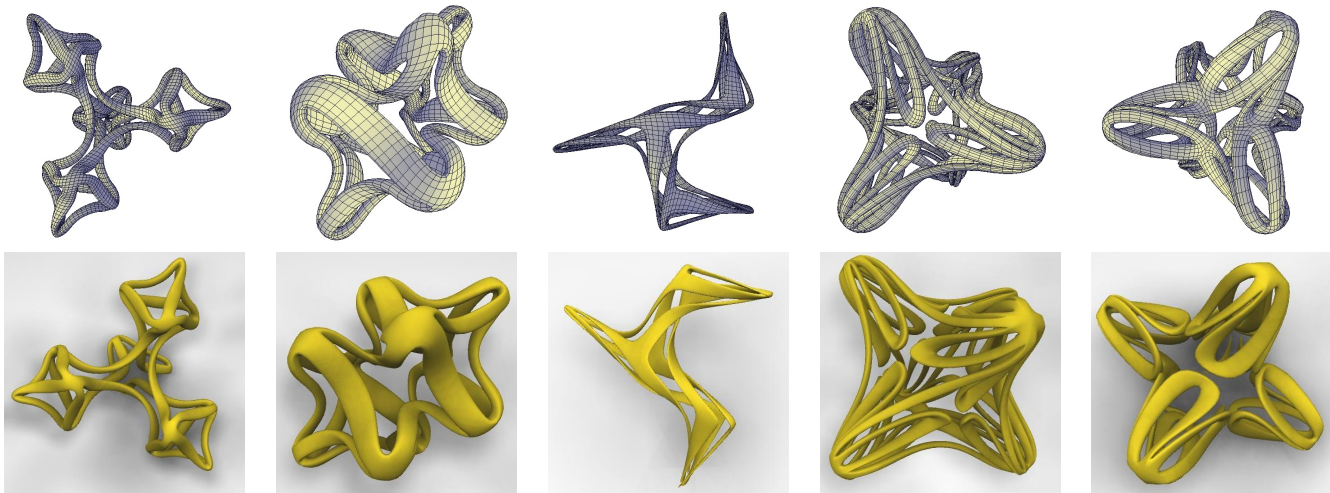


Figure 11. More complicated Twirling sculptures, all created with the approach presented in this paper. The structure of the shapes is visible even when we do not show the underlying mesh structure.

7. Conclusion and Future Work

In this paper, I have presented an approach for constructing aesthetically pleasing shapes. Because every face of a manifold can be given a consistent rotation order, one can apply an extrusion to each face of an associated manifold mesh using the same rotation and scaling factors in such a way that the edges of the original mesh are converted to S-shaped regions that consist of spiral arms. I have shown that it is possible to isolate these S-shaped regions using Doo-Sabin subdivision. Once the regions are isolated, it is possible to emphasize the twirling nature of these sculptures by opening S-shaped holes using Rind modeling.

In this paper, I have experimented with only a few of the many possible sculptural forms. Using the same approach a wider variety of sculptural forms can be created. For example, other extrusions such as 'Platonic extrusions' [22] can be applied.

The methods described in this paper are not the only way to make S-shaped regions visible. For example, instead of using just 2 colors to color the regions, we can use 3 or 4 colors. It is also possible to extrude to 3 or more different depths. We can even extrude some regions and poke holes in others. S-shaped regions can also be made visible if the extruded polygons of the initial mesh are cross or star shaped non-convex polygons. It is easy to create cross or star shapes inside of convex polygons (See the first row of Figure 12). If these non-convex polygons are extruded, the S-shaped spiral regions will be clearly visible in the resulting sculpture as shown in the second row of Figure 12.

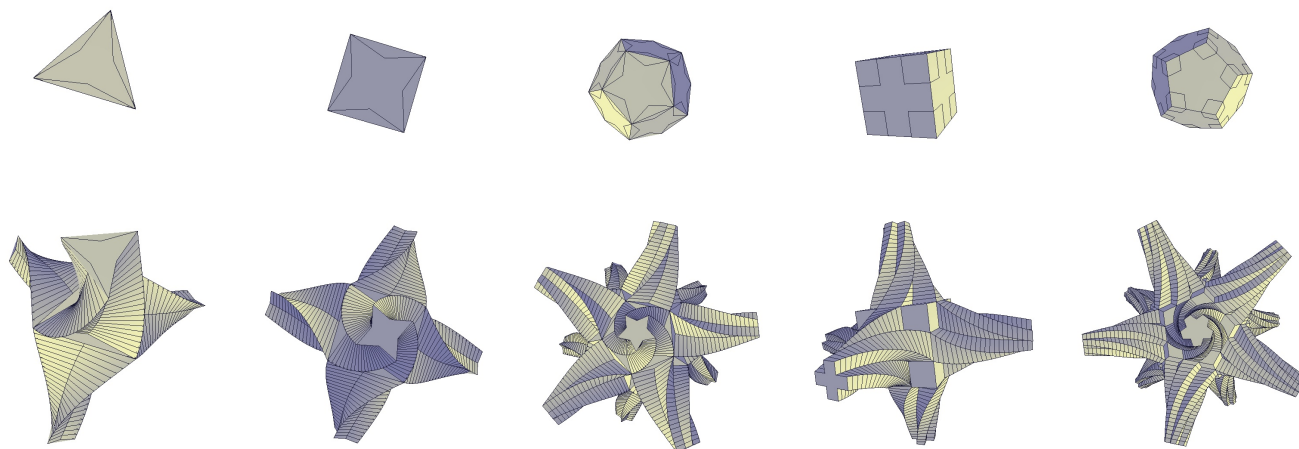


Figure 12. Creation and extrusion of non-convex polygons to make S-shaped regions sculpturally visible.

8. Acknowledgements

I am thankful to anonymous reviewers and the editor for their extremely helpful suggestions.

References

- [1] E. Akleman. Viza 657 - computer aided sculpting - twirling project. www-viz.tamu.edu/courses/viza657/06fall/projects/pr01.php, 2006.
- [2] E. Akleman and J. Chen. Guaranteeing the 2-manifold property for meshes with doubly linked face list. *International Journal of Shape Modeling*, 5(2):149–177, 1999.
- [3] E. Akleman and J. Chen. Regular meshes. In *Proceedings of Solid Modeling and Applications*, pages 213–219, 2005.
- [4] E. Akleman, J. Chen, and V. Srinivasan. A minimal and complete set of operators for the development of robust manifold mesh modelers. *Graphical Models Journal, Special issue on International Conference on Shape Modeling and Applications 2002*, 65(2):286–304, 2003.
- [5] E. Akleman, J. Chen, V. Srinivasan, and F. Eryoldas. A new corner cutting scheme with tension and handle-face reconstruction. *International Journal of Shape Modeling*, 7(2):111–121, 2001.
- [6] E. Akleman, V. Srinivasan, and J. Chen. Interactive rind modeling. In *Proceedings of International Conference on Shape Modeling and Applications*, pages 23–31, 2003.
- [7] E. Catmull and J. Clark. Recursively generated b-spline surfaces on arbitrary topological meshes. *Computer Aided Design*, (10):350–355, 1978.
- [8] Robert A. Dixon. *Mathographics*. Dover Publications Inc., 1991.
- [9] D. Doo and M. Sabin. Behavior of recursive subdivision surfaces near extraordinary points. *Computer Aided Design*, (10):356–360, 1978.
- [10] J. Edmonds. A combinatorial representation for polyhedral surfaces. *Notices American Mathematics Society*, (7):1960, 646.
- [11] David Eppstein. The geometry junkyard: Spirals. www.ics.uci.edu/~eppstein/junkyard/spiral.html, 2006.
- [12] Daniel Erdelyi. Some surprising properties of the spidrons. In *Bridges'2005, Mathematical Connections in Art, Music and Science*, pages 179–186, 2005.
- [13] Daniel Erdelyi. Spidron domain: The expending spidron universe. In *Bridges'2006, Mathematical Connections in Art, Music and Science*, pages 549–550, 2006.
- [14] H. Ferguson, A. Rockwood, and J. Cox. Topological design of sculptured surfaces. In *Proceedings of SIGGRAPH 1992, Computer Graphics Proceedings, Annual Conference Series*, pages 149–156. ACM, ACM Press / ACM SIGGRAPH, 1992.
- [15] Helaman Ferguson. Sculptures. www.helasculpt.com, 2006.
- [16] Hartmut Frommert and Christine Kronberg. Spiral galaxies. www.seds.org/messier/spir.html, 2006.
- [17] Bathsheba Grossman. Sculptures. www.bathsheba.com/, 2006.
- [18] B. Grunbaum. *Convex Polytopes*. pages 236–237, Springer-Verlag, New York, Inc., 2003.
- [19] George Hart. Conway notation for polyhedra. www.georgehart.com/virtual-polyhedra/conway_notation.html, 2006.
- [20] George Hart. Sculptures. www.georgehart.com, 2006.
- [21] Jurgen Koller. Spirals. www.mathematische-basteleien.de/spiral.htm, 2006.
- [22] E. Landreneau, E. Akleman, and V. Srinivasan. Local mesh operations, extrusions revisited. In *Proceedings of the International Conference on Shape Modeling and Applications*, pages 351–356, 2005.
- [23] B. Mandelbrot. *The Fractal Geometry of Nature*. W. H. Freeman and Co., New York, 1980.
- [24] M. Mantyla. *An Introduction to Solid Modeling*. Computer Science Press, Rockville, Ma., 1988.
- [25] Charles Perry. Sculptures. www.charlesperry.com/, 2006.
- [26] Ivars Peterson. Mathtrek: Pursuing pursuit curves. www.maa.org/mathland/mathtrek.7.16.01.html, July 16, 2001.
- [27] Rinus Roelofs. Sculptures. www.rinusroelofs.nl, 2006.
- [28] M. Sabin. Subdivision: Tutorial notes. Shape Modeling International 2001, Tutorial, May 2000.
- [29] Carlo Sequin. Sculptures. www.cs.berkeley.edu/~sequin/, 2006.
- [30] John Sharp. In pursuit of pursuit curves. In *ISAMA'99, First Interdisciplinary Conference of The International Society of The*

Arts, Mathematics and Architecture, pages 549–550, 1999.

- [31] I. Stewart. *Game, Set and Math: Enigmas and Conundrums*. Penguin Books, London, 1991.
- [32] D’Arcy Wentworth Thompson. *On Growth and Form (Originally Published in 1917)*. Dover, 1992.
- [33] Rowland Todd. Manifold. From MathWorld – A Wolfram Web Resource, created by Eric W. Weisstein. mathworld.wolfram.com/Manifold.html, 2008.
- [34] Official TopMod Website. Topological modeling software. www.topmod3d.org, September, 2007.
- [35] Eric W. Weisstein. Cornu spiral. From MathWorld – A Wolfram Web Resource, created by Eric W. Weisstein. mathworld.wolfram.com/CornuSpiral.html, 2008.
- [36] Eric W. Weisstein. Edge coloring. From MathWorld – A Wolfram Web Resource, created by Eric W. Weisstein. mathworld.wolfram.com/EdgeColoring.html, 2008.
- [37] Eric W. Weisstein. Spirals. From MathWorld – A Wolfram Web Resource, created by Eric W. Weisstein. <http://mathworld.wolfram.com/Spiral.html>, 2008.
- [38] Eric W. Weisstein. Surface. From MathWorld – A Wolfram Web Resource, created by Eric W. Weisstein. mathworld.wolfram.com/Surface.html, 2008.